Chemical Science

ROYAL SOCIETY OF CHEMISTRY

EDGE ARTICLE

View Article Online
View Journal | View Issue

Cite this: *Chem. Sci.*, 2025, **16**, 191

All publication charges for this article have been paid for by the Royal Society of Chemistry

Chemical protein synthesis combined with protein cell delivery reveals new insights on the maturation process of SUMO2†

Dana Shkolnik,‡[a] Subhasis Dey,‡[a] Mahdi Hasan,[a] Michael J. Matunis[b] and Ashraf Brik *[a]

The Small Ubiquitin-like Modifier (SUMO) is a crucial post-translational modifier of proteins, playing a key role in various cellular functions. All SUMOs are synthesized as precursor proteins that must be proteolytically processed. However, the maturation process of cleaving the extending C-terminal tail, preceding SUMOylation of substrates, remains poorly understood, especially within cellular environments. Chemical protein synthesis coupled with cell delivery offers great opportunities to prepare SUMO analogues to investigate this process *in vitro* and in live cells. Applying this unique combination we show that SUMO2 analogues containing the native tail undergo rapid cleavage and nuclear localisation, while a Gly93Ala mutation impairs cleavage and alters localisation. Tail mutations (Val94Glu, Tyr95Ala) affected cleavage rates, highlighting roles in SUMO–SENP protease interactions. In cells, SUMO2 analogues containing tail mutations underwent cleavage and subsequently incorporated into promyelocytic leukemia nuclear bodies (PML-NBs). These findings advance our understanding of SUMO2 maturation and provide a foundation for future studies of this process for different SUMO paralogues in various cell lines and tissues.

Received 15th September 2024
Accepted 7th November 2024

DOI: 10.1039/d4sc06254j

rsc.li/chemical-science

Introduction

Small Ubiquitin-like Modifier (SUMO) proteins are pivotal post-translational modifiers (PTMs) that regulate various cellular processes through their covalent conjugation mainly to lysine residues and also to N-terminal amine of target proteins across eukaryotes.[1–4] Mammals harbour five genes encoding SUMO paralogues (SUMO1–5)[5–7]—each has specialised roles in modulating substrate activity, subcellular localisation, and stability.[8–10] SUMO2 and SUMO3 share a remarkable 97% sequence similarity and are collectively termed SUMO2/3 and exhibit 47% similarity with SUMO1. SUMOylation, similar to ubiquitylation, is a highly regulated dynamic process mediated by an enzymatic cascade involving an E1 activating enzyme, E2 conjugating enzyme, and E3 ligase to conjugate SUMO with the substrate.[11] SUMOylation is a reversible PTM, regulated by SUMO-specific proteases (SENPs: SENP1–3, SENP5–7).[12] SENPs deSUMOylate substrates to maintain dynamic protein interaction networks.

SUMO proteins are highly conserved across species and are initially expressed as immature precursors with C-terminal extensions of 2–11 amino acids following the conserved Gly–Gly (GG) motif, known as tail. The single gene of SUMO expressed in yeast, Smt3, contains the ATY tail[13] and the five mammalian SUMO paralogues contain different tails, altered both in size and amino acid compositions. Interestingly, SUMO tails also vary across orthologues and paralogues, for instance, in most species, SUMO2 proteins feature the tail sequence 'Val–Tyr', whereas in some species (*e.g.*, snakes) other amino acids, such as the 'Met–Asn', are present (ESI, Section 12†). Mammalian precursors are processed by the same SENP proteases that remove SUMO from modified substrates. SENPs cleave the C-terminal extensions of SUMOs to expose the GG motif, a prerequisite step for SUMOylation. Various studies indicate that SENP family members exhibit distinct subcellular localisation and specificity. The specificity of SENP enzymes for SUMO paralogues in the maturation process is achieved through several structural and biochemical mechanisms.[14–16]

While there is ample experimental support on the SUMOylation pathway and the modifications by other ubiquitin-like (Ubl) modifiers in general, only a few studies have focused on the maturation process of SUMO precursors. For example, a previous study described the residue specificity of the *S. cerevisiae* SUMO protease Ulp1 against the (Gly–Gly↓Ala) positions of Smt3 and demonstrated that the conserved GG motif is not strictly required for its maturation.[17] In another study, it was

[a]*Schulich Faculty of Chemistry, Technion Israel Institute of Technology, Haifa, 3200008, Israel. E-mail: abrik@technion.ac.il*

[b]*Department of Biochemistry and Molecular Biology, Johns Hopkins University, Bloomberg School of Public Health, Baltimore, Maryland, USA*

† Electronic supplementary information (ESI) available. See DOI: https://doi.org/10.1039/d4sc06254j

‡ The authors have contributed equally.

shown that replacing the C-terminal tail residues following 'GG' in SUMO1 and -2 with that of SUMO3 affects the maturation efficiency.[18] Additionally, this study highlighted that the two amino acids immediately after the GG motif are crucial for paralogue specificity. Furthermore, structural studies demonstrated that selectivity in maturation is determined by electrostatic complementarity between the interacting regions in SENP1 and SENP2 with the SUMO paralogue tails.[16] A hydrophobic region in SENP2 is complementary to the SUMO2 tail, while a strongly acidic region in SENP1 interacts with the positively charged tail of SUMO1.

Nevertheless, various questions on the impact of mutations of the GG motif and tail region in SUMO precursors remain unexplored. In addition, we still lack *in vivo* data on the localisation of SUMO precursors compared to the mature forms, the dynamics of the maturation process, as well as the specific SENPs that are involved and how they are affected by cellular stress. Detailed studies on these aspects and others could provide valuable insights into the rationale behind the C-terminal tail and for targeting the SUMO machinery in drug development.

Total chemical synthesis and semi-synthesis of proteins enable selective modifications of both natural and unnatural components providing a significant opportunity to generate custom proteins for functional studies.[19] Yet, the studies of these synthetic proteins remain to be conducted in an *in vitro* setting excluding knowledge of their cellular behaviours. On the other hand, delivering these proteins with minimal cellular stress offers unique opportunities to study them in their native environment. Recently, we began to explore these combinations to shed light on unknown aspects of Ub, and Ub-like modifiers in live cells with efforts to overcome many challenges in these complex studies, in the delivery step, the monitoring process as well as in the data analysis.[20–24]

Studying the maturation process of endogenous SUMO proteins is challenging because it is highly dynamic and difficult to monitor within live cells. In this study, we harnessed the power of protein synthesis and protein cell delivery[19] to assess the SUMO maturation process *in vitro* and in live cells. We designed and synthesized ten different SUMO2 analogues to study the maturation process focusing on new aspects in a cellular context. Our results revealed, for the first time, a rapid tail cleavage of SUMO2 precursors in live cells. Our studies also investigated the impact of processing on the nuclear localisation of mature SUMO2 compared to the precursor, and the critical role of Gly93 in this process.

Results and discussion

To answer fundamental questions regarding the maturation process, we synthesized a focused library of SUMO2 proteins with different modifications, each of them with a specific rationale to gain further insights into this process. One major advantage of synthesizing SUMO is the ability to attach a small organic fluorophore to the synthetic protein. This modification allows tracking of the protein in live cell experiments, without interfering with its function. Numerous studies show that N-terminal tags attached to SUMO are well tolerated.[21,25,26] We combined two quick and straightforward methods, linear Solid Phase Peptide Synthesis (SPPS) and Multiplex Bead Loading (MBL).[21] Linear SPPS enabled us to synthesize SUMO proteins with site-specific modifications, while MBL facilitated the efficient delivery of multiple synthetic proteins into the same cell. These strategies supported live-cell studies, focusing on the localisation and conjugation of the synthesized SUMO2 analogue with respect to the maturation step.

SUMO proteins and their conjugated forms were prepared by different groups using either linear SPPS or ligation approaches.[21,27–32] In this study the set of SUMO2 protein analogues was synthesized using linear Fmoc-SPPS on 2-chlorotrityl chloride (2-CTC) resin, producing after cleavage the native carboxylic acid at the C-terminus. During the synthesis,

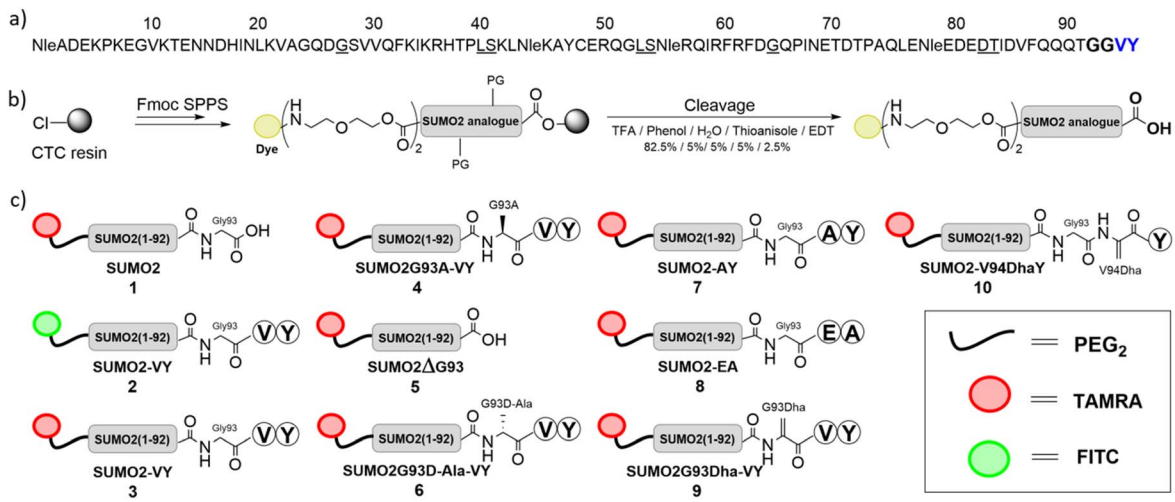

Fig. 1 Schematic presentation of the synthesis of labelled SUMO2 analogues: (a) the sequence of SUMO2, where the pseudoproline dipeptides and Gly(Dmb) positions are underlined. The native SUMO2 tail is highlighted in blue. (b) General synthesis scheme for SUMO2 analogues **1–10**. (c) The labelled synthetic SUMO2 analogues used in this study.

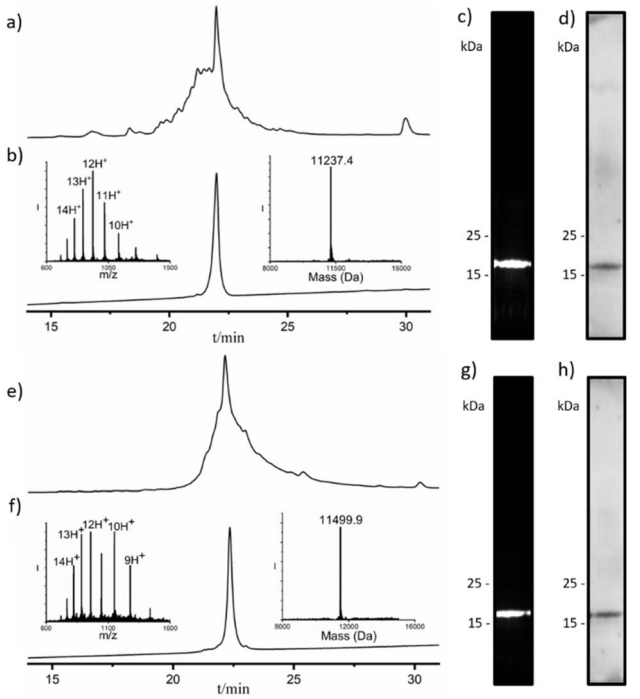

Fig. 2 Characterization of synthetic SUMO2 analogues, **1** and **3**. (a) Analytical HPLC chromatogram of crude **1**. (b) Analytical HPLC and ESI-MS of purified **1** (observed mass 11 237.4 ± 0.3 Da, calcd 11 238.6 Da). (c) SDS-PAGE analysis of **1** using TAMRA channel. (d) WB analysis of **1** using SUMO2 antibody. (e) Analytical HPLC chromatogram of crude **3**. (f) Analytical HPLC and ESI-MS analysis of purified **3** (observed mass 11 499.9 ± 0.5 Da, calcd 11 500.9 Da). (g) SDS-PAGE analysis of **3** in TAMRA channel. (h) WB analysis of **3** using SUMO2 antibody.

we introduced three pseudoproline dipeptides and Gly dimethoxybenzyl (DMB) at two positions to achieve better synthesis with improved yields (Fig. 1a).[28] In the SUMO2 sequence, Met residues were substituted with Nle, a widely used mutation in chemical protein synthesis reported across various studies to avoid Met oxidation which could complicate purification.[33–35] Our previous study on SUMO2 demonstrated that this mutation did not alter the protein function or localisation in the cells.[21,29] Following the complete synthesis of the protein sequence, two PEG molecules were attached to the N-terminus to serve as a linker between the protein sequence and the relative organic fluorophore (Fig. 1b and c). Initially, we synthesized SUMO2 without its tail (**1**) and with the native tail, VY, having fluorescein (FITC) (**2**) or 5-carboxytetramethylrhodamine (TAMRA) (**3**) to follow conjugation and cellular localisation studies. The use of different organic dyes for proteins **1** and **2** permitted their co-delivery to the same cells *via* MBL and allowed comparison. Purification and characterization of the analogues were performed through RP-HPLC, mass spectrometry, fluorescence gel analysis using the TAMRA channel, and western blot (WB) using SUMO2 antibody (Fig. 2a–h).

With these proteins in hand, we first investigated the localisation of SUMO2 analogues, **1** and **2**, at three time points (15 minutes, one hour, and three hours) following protein delivery. The analogues were delivered into U2OS cells using the MBL approach in a final concentration of 2 μM for each protein. Subsequently, cells were incubated at 37 °C for 15 minutes, one hour, and three hours, then were imaged using laser scanning confocal microscopy (LSCM) in the TAMRA and FITC channels. At the initial time point (15 minutes), proteins **1** and **2** exhibited nearly identical localisation, predominantly accumulating in the nucleus (Fig. 3a). This localisation remained consistent throughout all the measured time points. The observed localisation of both analogues suggests rapid tail cleavage, in which **1** and **2** become identical proteins that share the same intracellular behaviour following delivery.

Based on the observed localisation, we examined the conjugation pattern of analogues **1** and **3** to test our assumption that the tail was rapidly cleaved to allow conjugation. Analogues **1** and **3** were delivered into U2OS cells at 5 μM final concentration and incubated for the same time points as the localisation experiments (15 minutes, 1 hour, and 3 hours). Subsequently, cells were lysed using 2× Laemmli sample buffer and analysed by SDS-PAGE. At the earliest 15 minute time point, and at later time points, analogues **1** and **3** exhibited similar high molecular weight bands, consistent with rapid and efficient tail processing and conjugation to protein substrates (Fig. 3b). These results showed a rapid tail cleavage for the first time in live cells.

To further validate these results, we expressed and purified the SENP2 active domain, which cleaves the SUMO2 tail *in vitro*,[14,27] and utilized it to investigate the maturation process. We performed an *in vitro* assay in which the SENP2 active domain (40 nM) was incubated at 37 °C with 5 μM of SUMO2 analogue **3**. Our result indicated that the tail of the SUMO analogue was cleaved (>90%) within 15 minutes (Fig. 3c).

Motivated by these findings, we set out to design a SUMO2 analogue **4** with an uncleavable tail. Relying on previous reports that substitution of Gly to any larger amino acid may affect SUMO–SENP interactions due to the constricted hydrophobic tunnel of the SENP catalytic site,[15] we substituted Gly93 of SUMO2 to Ala to produce analogue **4**. This analogue was prepared using the procedure mentioned in the general synthetic scheme (Fig. 1). In addition, a SUMO2 analogue with deletion of Gly93 and the C-terminal tail, SUMO2ΔG93 (**5**), was synthesized to serve as a control for an unconjugatable SUMO2.[36]

Before initiating cellular experiments with analogue **4**, *in vitro* reactions were conducted to test the hypothesis that the Gly93 to Ala substitution inhibits processing by SENP2. Our results clearly showed that the tail in analogue **4** was completely stable after three hours of incubation with SENP2 (Fig. S10a†). With these results in hand, we checked the localisation of analogue **4**, which revealed localisation in the nucleus and the cytoplasm that differs from analogues **1** and **2** which were restricted to the nucleus. The uncleavable analogue **4** showed very similar localisation as the unconjugatable SUMO2 analogue **5** (Fig. 4a). These findings highlight the effect of tail processing and subsequent covalent protein modification on accumulation of SUMO2 in the nucleus. The connection between localisation and protein modification was supported by fluorescence gel analysis, in which high molecular weight

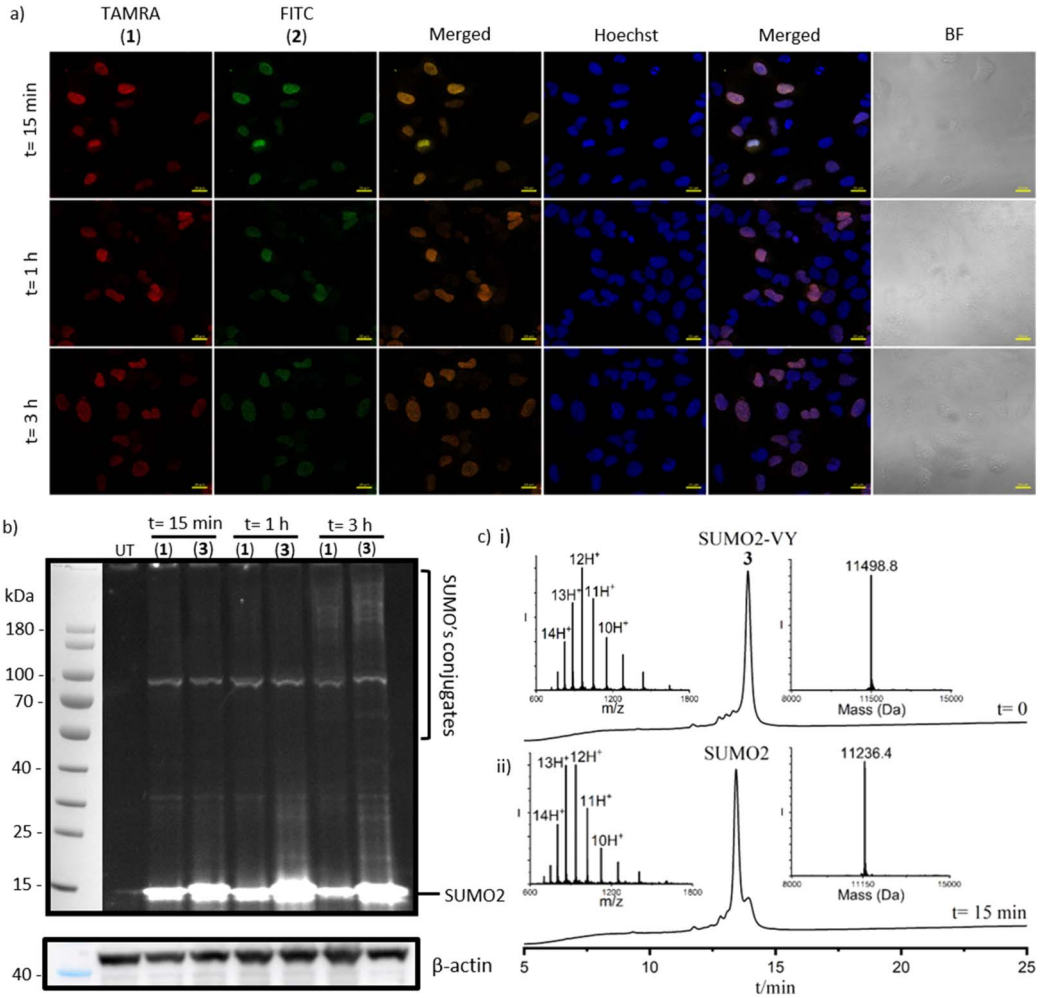

Fig. 3 (a) LSCM images for the time-lapse experiment of U2OS cells loaded with 2 μM of **1** (TAMRA, red), **2** (FITC, green), and Hoechst nuclear stain (blue). Time-lapse imaging was taken following protein delivery in 15 min, 1 h, and 3 h. Scale bars are 20 μm. This experiment was repeated three times independently. (b) Fluorescence gel analysis of U2OS cells treated either with 5 μM of **1** or **3**, which were lysed at three different time points (15 min, 1 h, and 3 h) after protein delivery. Each lane refers to a different analogue. UT represents the untreated samples. This experiment was repeated three times independently. (c) HPLC and ESI-MS analysis of the *in vitro* reaction between expressed SENP2 active domain and **3**. (i) $t = 0$ represents analogue **3** alone (observed mass 11 498.8 ± 0.5 Da, calcd 11 500.9 Da) (ii) $t = 15$ min represents the reaction between **3** and SENP2 after 15 minutes of incubation (observed mass 11 236.4 ± 0.3 Da, calcd 11 238.6 Da). This experiment was repeated three times independently.

protein conjugates of analogues **4** and **5** were not detected (Fig. 4b). Together, these findings demonstrate that mutating the conserved Gly93 to Ala abolishes the cleavage process and results in a unique localisation pattern of immature SUMO2. This effect on localisation suggests that the covalent conjugation of SUMO2 to proteins in the nucleus affects its nuclear–cytoplasmic distribution. The significant impact of mutating Gly93 to Ala on the cleavage process may stem from the narrow tunnel through which the SUMO2 C-terminus must enter for cleavage.[15] Such a step can be impeded by any structural changes or the mispositioning of the scissile bond of SUMO2 towards the active site Cys.

To further expand our understanding of the inhibition of the cleavage process when mutating Gly93 to Ala, we synthesized analogue **6** in which this Gly was mutated to D-Ala. Such a mutation could change the dihedral angle of the scissile peptide bond and possibly allow the cleavage to proceed since D-Ala has been proposed to be a mimic of Gly.[37] Analysis of the *in vitro* reaction between SENP2 and analogue **6** revealed that the cleavage also did not proceed with this analogue even after three hours of incubation (Fig. S10b†), suggesting the important role of the narrow tunnel in the preference of the Gly–Gly motif. Previous structural study of the SENP2 catalytic domain in complex with SUMO2 precursor showed that the tail (VY) kinks at Gly92, positioned the GG motif over Trp410 of SENP2.[38] Mutation of Trp410 to Ala reduced activity in processing, underscoring its role in positioning the SUMO diglycine motif and scissile bond at the active site. Therefore modifying Gly93 with any larger amino acid could affect the positioning of the scissile bond due to steric clashes with Trp410 and restrict its entry to the catalytic site, which is reflected in our results regarding the inhibition of processing analogues **4** and **6**.

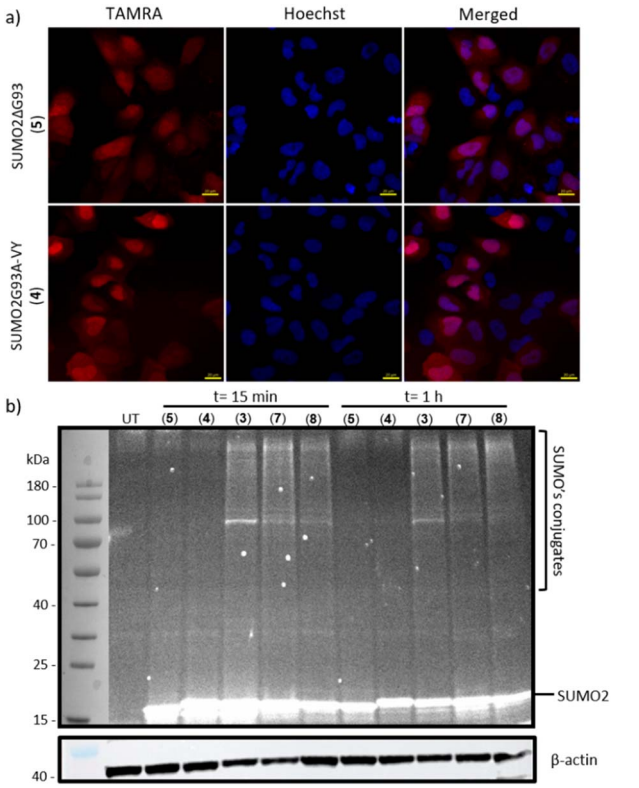

Fig. 4 (a) LSCM images of fixed U2OS cells loaded with 2 μM of either **5** or **4** (red, TAMRA). Hoechst was used as a nuclear stain (blue). Fixation was done after 1 h of the protein delivery. Scale bars are 20 μm. This experiment was repeated three times independently. (b) Fluorescence gel analysis of U2OS cells loaded with **3**–**5**, **7**, and **8**, where each lane refers to a different analogue. Cells were treated with MG132 for 4 h before protein delivery and then lysed after 15 min or 1 h. UT represents the untreated samples. This experiment was repeated three times independently.

After demonstrating the impact of altering the position preceding the C-terminal tail on the cleavage process, we further examined whether changes in the tail itself would affect the cleavage reaction. Previous studies have primarily focused on generating SUMO chimeras, such as SUMO2 fused with the tail of SUMO3 or *vice versa*.[14,15,18] These studies showed that the maturation efficiencies of SUMO2 containing the SUMO3 tail are comparable to those of SUMO3.[15,18] The first two amino acids following the GG motif are critical in regulating maturation efficiency.[15] Another study demonstrated that the tail region is essential for defining the endopeptidase specificity of SENPs, allowing for the discrimination between pro-SUMO2 and pro-SUMO3.[14] Our study extends this research by exploring alternative tail compositions beyond those amino acids that are present in the native SUMO paralogues. We initially prepared SUMO2-AY (**7**) (SUMO2-Ala94–Tyr95). The reason for mutating Val94 to Ala in the tail was based on the significant impact observed upon replacing Gly93 with Ala. Our gel analysis results after cell delivery and lysis showed high molecular conjugates for analogue **7** at both the 15 minutes and 1 hour time points (Fig. 4b). Despite challenges in the quantification of conjugation levels due to variations in protein analogue delivery to cells by bead loading, our results suggest that the Val94 to Ala substitution did not significantly affect cleavage and subsequent conjugation.

To further investigate flexibility in changing the tail composition, we synthesized, SUMO2-EA (**8**) (SUMO2-Glu94–Ala95). This analogue features completely different C-terminal tail residues in terms of polarity and hydrophobicity to those in SUMO2 and in SUMO1 and SUMO3. The *in vitro* processing rate of analogue **8** with SENP2 was slower compared to analogues **3** or **7** (Fig. 3c, S10c and d†). Despite its slower processing *in vitro*, analogue **8** showed conjugation to proteins in cells within 15 minutes (Fig. 4b). Our findings align with a previous study[16] which showed that the region within SENP2 interacting with the SUMO C-terminus is hydrophobic and has a preference for hydrophobic amino acids such as valine over glutamic acid. Based on our findings, it is evident that substitutions in Gly93 preceding the tail (*e.g.* analogues **4** and **6**) inhibit the cleavage process, whereas mutations within the tail (analogues **7** and **8**) do not abolish the process but rather affect its rate. These findings are consistent with the previously resolved SENP2–SUMO2 precursor crystal structure,[38] wherein the tail is oriented toward the SENP2 surface comprised of residues Trp410, Val477, Gly545, and Met497, which exhibits a preference for hydrophobic amino acids. These interactions likely underlie the observed differences in the *in vitro* processing rates between the VY, AY, and EA tails. The Val94Glu mutation disrupts these hydrophobic interactions, leading to the reduced observed rate.

Understanding the interaction between SUMO proteins and the enzymes responsible for tail cleavage is crucial for elucidating the SUMO processing step. While previous *in vitro* studies have examined the distinct processing activities of different SENPs on SUMO paralogs,[15,18,38] demonstrating that electrostatic interactions account for the selectivity between the C-terminal tail and the specific SENP,[15] information is still lacking in live cells. Of particular importance, the exact SENPs responsible for processing SUMOs *in vivo* remain unknown. To address this gap, we aimed to synthesize a SUMO2 activity-based probe having dehydroalanine (Dha), as an electrophile to capture the cellular-specific maturation enzymes.

Inspired by our previous study for trapping the catalytic Cys residue of a specific deubiquitinating enzyme (DUB) in the ubiquitination process, we positioned the Dha moiety near the scissile amide bond[39–41] to generate the SUMO2-Gly93Dha-tail probe. To construct this probe, we mutated Gly93 to Cys during SPPS of SUMO2 and replaced the internal Cys48 with Ser. Finally, to convert the Cys to Dha, this SUMO derivative was treated with α,α′-dibromo-adipyl(bis)amide to give the desired SUMO2-activity-based probe analogue **9** in 22% isolated yield (Fig. S9†).

Delivery of analogue **9** to live cells showed low reactivity towards endogenous enzymes. Unfortunately, this probe failed to capture any enzyme and did not exhibit any conjugation, suggesting that the tail remained intact (Fig. 5a and S10e†). Two main factors may account for the failure to capture any SENP using this probe. One possibility could be attributed to the steric hindrance caused by the planar double bond group

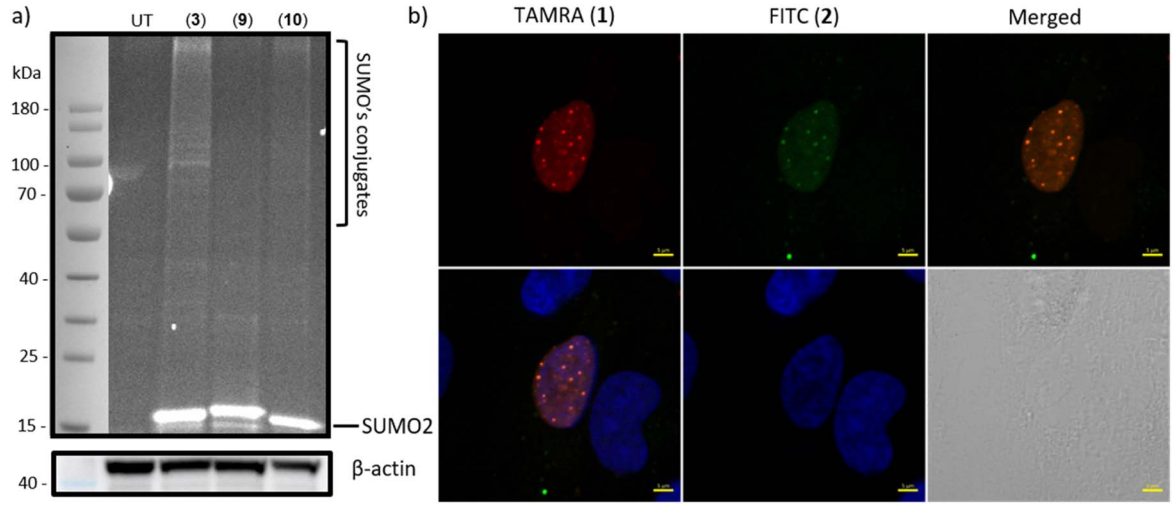

Fig. 5 (a) Fluorescence gel analysis of U2OS cells loaded either with analog **3** (serve as a control), or with probes **9**, **10**. Where each lane refers to a different analogue. Cells were lysed after 1 h of the protein delivery. UT represents the untreated samples. This experiment was repeated three times independently. (b) LSCM images of fixed U2OS cells loaded with 2 μM of **1** (TAMRA, red), **2** (FITC, green), and Hoechst nuclear stain (blue). Fixation was done 1 h after protein delivery. Scale bars are 5 μm. This experiment was repeated three times independently.

within the narrow tunnel of SENPs, like the Ala case in analogue **4**. Another explanation could relate to the positioning of the Dha, whereby the electrophilic group may be located far from the catalytic Cys of SENPs. Indeed, a previous study reported by Reverter *et al.* also failed to capture SENP2 and SENP7 with a similar Dha probe *in vitro*.[42]

This prompted us to alter the position of the Dha from Gly93 to Val94, hoping to change the proximity of this reactive moiety to the catalytic Cys. We generated SUMO2 activity-based probe **10** and subjected it to *in vitro* processing assays with SENP2. The cleavage reaction and the gel fluorescence assay revealed that this probe underwent cleavage at the expected site, leading to the removal of the Dha as part of the tail, rather than reacting with the enzyme (Fig. 5a and S10f†).

Although alternative reactive groups are available in the literature[43] and can be introduced in the C-terminus of the immature SUMO, they may not capture solely the maturation enzymes and are prone to be cleaved with the tail. Additionally, the short length of the tail limits the options available for modification. Nevertheless, these results obtained from probes **9** and **10** again highlight the sensitivity of the changes in Gly93 and the flexibility of the tail composition.

Next, we wanted to evaluate the effect of cleavage of the SUMO2 tail on its incorporation into PML-NBs, which are dependent on SUMOylation for their formation and function.[44–46] These NBs are localised inside the nucleus where SUMO2 exists in its conjugated form. Detection of PML-NBs would indicate that SUMO2 has been processed and conjugated to PML and associated PML-NB substrates. Our initial analysis with analogues **1** and **2** suggested a localisation of conjugatable SUMO2 to PML-NBs (Fig. 3a). Here, we analysed cells at higher resolution and included additional analogues. We loaded U2OS cells with our synthesized SUMO2 analogues **1**, **2**, and **4–8**, followed by incubation for an hour. Cells were subsequently fixed and examined by LSCM. The images obtained by LSCM clearly showed the incorporation of analogues **1**, **2**, **7**, and **8** into nuclear foci with the expected spherical shape of PML-NBs[47] (Fig. 5b and S11†). On the other hand, SUMO2 analogues **4–6** were not observed in nuclear foci, demonstrating that processing and conjugation are required for PML-NB localisation (Fig. S11†).

Conclusions

Using chemical protein synthesis and cell delivery we presented a detailed analysis of the maturation process of SUMO2 precursor protein both under *in vitro* and cellular conditions. To the best of our knowledge, this is the first study of the maturation process in live cells, revealing new insights into various aspects of this process. Our findings demonstrated that SUMO2 with the native tail underwent rapid cleavage, leading to nuclear localisation and concentration in PML-NBs. In contrast, a Gly93Ala substitution impaired cleavage and altered localisation patterns, highlighting the critical role of Gly93 in tail cleavage and the influence of conjugation to protein substrates on SUMO2 localisation. The exact mechanisms affecting the concentration of SUMO2 in the nucleus are not well understood. The even distribution of uncleavable and unconjugatable SUMO2 between the cytoplasm and the nucleus (analogues **4** and **5**) suggests that nuclear import may be passive, with covalent conjugation to proteins effectively trapping SUMO2 in the nucleus and within PML-NBs. The effect of mutations in the tail on SUMO2 processing was also tested. We found that while substitutions with residues of similar polarity as the native tail residues did not exhibit dramatic changes in the cleavage, mutations with residues of different polarity slowed the cleavage rate *in vitro* by SENP2. However, changes in the tail composition appeared to have much less effect on cleavage in the cellular environment. Overall, our findings pave the way for

future studies to investigate the functional significance of SUMO precursor processing and for analysis of different SUMO paralogues in various conditions, cell lines, and tissues.

Data availability

The data supporting this article have been included as part of the ESI.†

Author contributions

D. S. conducted the protein synthesis and the biochemical experiments, S. D. conducted the protein synthesis, S. D. and M. H. expressed and purified SENP2, S. D. and M. H. assisted with the biochemical experiments. M. J. M. discussed the ideas of the project. A. B. supervised all aspects of the project. All authors assisted in writing the manuscript and ESI.†

Conflicts of interest

There are no conflicts to declare.

Acknowledgements

A. B. holds the Jordan and Irene Tark Academic Chair. This research was supported by the United States – Israel Binational Science Foundation (BSF) (grant no. 2022228). M. H. acknowledges the support of the VATAT scholarship. Some of the figures were created with **https://www.biorender.com/**.

Notes and references

1 Z. Shen, P. E. Pardington-Purtymun, J. C. Comeaux, R. K. Moyzis and D. J. Chen, *Genomics*, 1996, **36**, 271–279.
2 M. J. Matunis, E. Coutavas and G. Blobel, *J. Cell Biol.*, 1996, **135**, 1457–1470.
3 E. S. Johnson, *Annu. Rev. Biochem.*, 2004, **73**, 355–382.
4 W. Weng, X. Gu, Y. Yang, Q. Zhang, Q. Deng, J. Zhou, J. Cheng, M. X. Zhu, J. Feng, O. Huang and Y. Li, *Nat. Commun.*, 2023, **14**, 5688.
5 Y. C. Liang, C. C. Lee, Y. L. Yao, C. C. Lai, M. L. Schmitz and W. M. Yang, *Sci. Rep.*, 2016, **6**, 1–15.
6 D. Guo, M. Li, Y. Zhang, P. Yang, S. Eckenrode, D. Hopkins, W. Zheng, S. Purohit, R. H. Podolsky, A. Muir, J. Wang, Z. Dong, T. Brusko, M. Atkinson, P. Pozzilli, A. Zeidler, L. J. Raffel, C. O. Jacob, Y. Park, M. Serrano-Rios, M. T. M. Larrad, Z. Zhang, H. J. Garchon, J. F. Bach, J. I. Rotter, J. X. She and C. Y. Wang, *Nat. Genet.*, 2004, **36**, 837–841.
7 H. L. Su and S. S. L. Li, *Gene*, 2002, **296**, 65–73.
8 S. Müller, A. Ledl and D. Schmidt, *Oncogene*, 2004, **23**, 1998–2008.
9 A. C. O. Vertegaal, *Nat. Rev. Mol. Cell Biol.*, 2022, **23**, 715–731.
10 U. Sahin, H. de Thé and V. Lallemand-Breitenbach, *Cells*, 2022, **11**, 1–24.
11 L. M. Lois and C. D. Lima, *EMBO J.*, 2005, **24**, 439–451.
12 C. M. Hickey, N. R. Wilson and M. Hochstrasser, *Nat. Rev. Mol. Cell Biol.*, 2012, **13**, 755–766.
13 E. S. Johnson, I. Schwienhorst, R. J. Dohmen and G. Blobel, *EMBO J.*, 1997, **16**, 5509–5519.
14 J. Mikolajczyk, M. Drag, M. Békés, J. T. Cao, Z. Ronai and G. S. Salvesen, *J. Biol. Chem.*, 2007, **282**, 26217–26224.
15 D. Reverter and C. D. Lima, *Structure*, 2004, **12**, 1519–1531.
16 L. N. Shen, C. Dong, H. Liu, J. H. Naismith and R. T. Hay, *Biochem. J.*, 2006, **397**, 279–288.
17 F. Zhang, H. Zheng, Y. Xian, H. Song, S. Wang, Y. Yun, L. Yi and G. Zhang, *Int. J. Mol. Sci.*, 2022, **23**, 12188.
18 Z. Xu and S. W. N. Au, *Biochem. J.*, 2005, **386**, 325–330.
19 G. Mann, P. Sadhu and A. Brik, *Acc. Chem. Res.*, 2022, **55**, 2055–2067.
20 G. Mann, G. Satish, P. Sulkshane, S. Mandal, M. H. Glickman and A. Brik, *Chem. Commun.*, 2021, **57**, 9438–9441.
21 G. Mann, P. Sadhu and A. Brik, *ChemBioChem*, 2022, **23**, e202200122.
22 M. Hasan, D. Panda, G. Mann and A. Brik, *ChemBioChem*, 2024, **25**, e20230073.
23 S. Mandal and A. Brik, *Chem. Commun.*, 2022, **58**, 8782–8785.
24 A. Brik, A. Saha, R. Mousa, Y. Alalouf, P. Sadhu, M. Hasan, S. Mandal and G. Mann, *Angew. Chem., Int. Ed.*, 2024, e202410135.
25 K. Drabikowski, J. Ferralli, M. Kistowski, J. Oledzki, M. Dadlez and R. Chiquet-Ehrismann, *Sci. Rep.*, 2018, **8**, 1–12.
26 F. Ayaydin and M. Dasso, *Mol. Biol. Cell*, 2004, **15**, 5208–5218.
27 T. G. Wucherpfennig, V. R. Pattabiraman, F. R. P. Limberg, J. Ruiz-Rodríguez and J. W. Bode, *Angew. Chem., Int. Ed.*, 2014, **53**, 12248–12252.
28 M. P. C. Mulder, R. Merkx, K. F. Witting, D. S. Hameed, D. El Atmioui, L. Lelieveld, F. Liebelt, J. Neefjes, I. Berlin, A. C. O. Vertegaal and H. Ovaa, *Angew. Chem.*, 2018, **130**, 9096–9100.
29 S. Mandal, G. Mann, G. Satish and A. Brik, *Angew. Chem., Int. Ed.*, 2021, **60**, 7333–7343.
30 J. Bouchenna, M. Sénéchal, H. Drobecq, J. Vicogne and O. Melnyk, *Bioconjugate Chem.*, 2019, **30**, 2967–2973.
31 E. Boll, H. Drobecq, N. Ollivier, L. Raibaut, R. Desmet, J. Vicogne and O. Melnyk, *Chem. Sci.*, 2014, **5**, 2017–2022.
32 S. Bondalapati, E. Eid, S. M. Mali, C. Wolberger and A. Brik, *Chem. Sci.*, 2017, **8**, 4027–4034.
33 L. Moroder, *J. Pept. Sci.*, 2005, **11**, 187–214.
34 S. Roosenburg, P. Laverman, L. Joosten, A. Eek, W. J. G. Oyen, M. De Jong, F. P. J. T. Rutjes, F. L. Van Delft and O. C. Boerman, *Bioconjugate Chem.*, 2010, **21**, 663–670.
35 L. Dery, P. S. Reddy, S. Dery, R. Mousa, O. Ktorza, A. Talhami and N. Metanis, *Chem. Sci.*, 2017, **8**, 1922–1926.
36 K. Yamada, M. Muramatsu, D. Saito, M. Sato-Oka, M. Saito, T. Moriyama and H. Saitoh, *Biosci., Biotechnol., Biochem.*, 2012, **76**, 1035–1037.
37 F. I. Valiyaveetil, M. Sekedat, R. MacKinnon and T. W. Muir, *Proc. Natl. Acad. Sci. U. S. A.*, 2004, **101**, 17045–17049.
38 D. Reverter and C. D. Lima, *Nat. Struct. Mol. Biol.*, 2006, **13**, 1060–1068.

39 N. Haj-Yahya, H. P. Hemantha, R. Meledin, S. Bondalapati, M. Seenaiah and A. Brik, *Org. Lett.*, 2014, **16**, 540–543.
40 R. Meledin, S. M. Mali, O. Kleifeld and A. Brik, *Angew. Chem.*, 2018, **130**, 5747–5751.
41 M. Jbara, S. Laps, M. Morgan, G. Kamnesky, G. Mann, C. Wolberger and A. Brik, *Nat. Commun.*, 2018, **9**, 3154.
42 Y. Li, N. Varejão and D. Reverter, *Nat. Commun.*, 2022, **13**, 1819.
43 X. Sui, Y. Wang, Y. X. Du, L. J. Liang, Q. Zheng, Y. M. Li and L. Liu, *Chem. Sci.*, 2020, **11**, 12633–12646.
44 T. H. Shen, H. K. Lin, P. P. Scaglioni, T. M. Yung and P. P. Pandolfi, *Mol. Cell*, 2006, **24**, 331–339.
45 S. Müller, M. J. Matunis and A. Dejean, *EMBO J.*, 1998, **17**, 61–70.
46 U. Sahin, H. De Thé and V. Lallemand-Breitenbach, *Nucleus*, 2014, **5**, 499–507.
47 F. M. Boisvert, M. J. Hendzel and D. P. Bazett-Jones, *J. Cell Biol.*, 2000, **148**, 283–292.